

Influence of Chemical and Spatial Constraints on the Structures of Inorganic Compounds

I. D. BROWN

Brockhouse Institute of Materials Research, McMaster University, Hamilton, Ontario, Canada L8S 4M1. E-mail: idbrown@mcmaster.ca

(Received 20 March 1996; accepted 7 February 1997)

Abstract

The restrictions imposed by both chemistry and three-dimensional space on the structures of inorganic crystals can be analysed using the bond-valence model and space-group theory. The bond-valence model is used to construct a bond graph (connectivity table) from which the multiplicities and possible site symmetries of each atom can be assigned. These are matched to Wyckoff positions of the three-dimensional space groups, selecting the matching space group with the highest possible symmetry. High-symmetry structures such as NaCl, perovskite and garnet are readily derived from the chemical formula and, with a little more effort, the same can be done for structures of intermediate symmetry such as wurtzite, corundum and rutile. For other compounds a relationship between the site symmetry and the multiplicity of an atom can severely restrict the possible structures.

1. Introduction

The bonding topology of every solid must conform to both the laws of chemistry and the restrictions of three-dimensional space. Unless both sets of constraints are satisfied the solid cannot exist. The interplay between them is the subject of this paper, the laws of chemistry being expressed through the bond-valence model of inorganic chemistry (Brown, 1992) and the laws of three-dimensional space expressed through the space-group theory of crystals (*International Tables for Crystallography*, 1983, Vol. A).

An inorganic crystal can be represented by an infinite network of atoms connected by bonds. The network, which must conform to one of the 230 three-dimensional space groups described in *International Tables for Crystallography* (1983, Vol. A), can be decomposed into two parts, the topology of the asymmetric unit and the symmetry operators of the space group. If both can be found separately, they can be combined to generate the infinite bond network.

The asymmetric unit, which describes short-range order, is determined by the laws of chemistry, namely the rules that determine which atoms bond to each

other. In practice, when analysing a structure, it is more convenient to start, not with the asymmetric unit, but with the chemical formula unit which may contain several asymmetric units if the atoms lie on special positions. Any crystallographic symmetry used by the formula unit must, of course, be part of the symmetry of the space group and, therefore, the compound can only crystallize in a space group that contains this symmetry. Hence, we find that the chemistry, which determines the short-range order, can influence the choice of space group which determines the long-range order. A careful examination of the chemistry can therefore be used to explore which space groups are compatible with the chemistry and thus what long-range order is possible.

For a given chemical composition, plausible local environments for each atom can be predicted using the bond-valence model. These are used to determine the symmetry and multiplicity of each atom in the formula unit and to find those space groups that have matching Wyckoff positions. An examination of the candidate space groups starting with those of highest symmetry can be used to explore possible structures and will, in many cases, show why a particular compound cannot adopt a high-symmetry structure. In all cases the procedure gives insights into the factors that determine the symmetry, space group and long-range order of different compounds.

To assist the reader, the salient features of the bond-valence model are reviewed in §2. The constraints introduced by space-group theory are derived in §3 and their application is described in §4. Finally, some worked examples are given in §5.

2. The bond-valence model

The recently developed bond-valence model allows inorganic crystal structures to be analysed in terms of the chemical bonding between nearest-neighbour atoms. Only the main features are summarized here since a full description of the model has been given by Brown (1992).

In the bond-valence model each atom in an inorganic solid is assigned an atomic valence (positive or

negative) which is normally equal to its oxidation state and each atom is connected by bonds to those nearest neighbours that have valences of opposite sign. Thus, the structure is represented by a network of atoms linked by bonds in which atoms with positive valence (cations) are bonded only to atoms with negative valence (anions) and *vice versa*. Each atom shares its valence as equally as possible among the bonds it forms, thereby associating with each bond a valence, whose sum around any atom is equal to its atomic valence. The bond valences, s , determined in this way are found to correlate with the bond lengths, R , according to

$$s = \exp[(R_0 - R)/B], \quad (1)$$

where R_0 and B are constants whose values have been determined empirically for most pairs of atoms that form bonds. Tabulations are given by Brown & Altermatt, (1985) and Brese & O'Keeffe, (1992). By analogy with the Kirchhoff laws for solving electrical networks, the bond valences can be determined from the bond network using the two network equations, (2) and (3), known, respectively, as the valence sum rule and the equal valence rule

$$\sum_j s_{ij} = V_i \quad (2)$$

$$\sum_{\text{loop}} s_{ij} = 0, \quad (3)$$

where V_i is the valence of atom i , s_{ij} is the valence of the bond between atoms i and j , and the summation in (3) is performed around any closed loop in the bond network. The solution to the two network equations corresponds to the valence of the atoms being distributed as uniformly as possible between the various bonds and, together with (1), it gives a unique prediction for the valence and length of each bond.

Equations (1)–(3) can provide a description of the geometry of a compound, but only if the bond network is known. However, it is not necessary to know the full bond network, only the short-range part, that is, the first-neighbour bonding environment which can be represented by a finite bond graph. First imagine that the long-range topology is known and that the structure is represented by a bond network that extends indefinitely in all directions. Extracting one or two chemical formula units from this infinite network requires the breaking of bonds, but, by reconnecting pairs of chemically equivalent broken bonds, a finite bond graph of the kind shown in the figures can be created. Although the information about the long-range topology, and hence the space group, is lost in this graph, the graph preserves information about the local environment of each atom, *i.e.* number of bonds it forms and the nature of its nearest neighbours. This information is sufficient to determine the ideal bond lengths using (1)–(3).

Since the finite graph involves only the local properties of the atoms, it can often be generated using simple chemical rules in the same way as the molecular

Table 1. Average observed coordination numbers and bonding strengths in valence units for selected atoms (from Brown, 1988)

	Atomic valence	Ligand	Coordination number	Bonding strength
Al	3	O	5.27	0.57
Ba	2	O	10.24	0.195
Ca	2	O, F	7.31	0.274
Cd	2	O	6.14	0.326
Cd	2	S	4.6	0.43
Cl	-1	All cations	6	0.167
Cs	1	Halogen	10.4	0.094
Cu	1	Halogen	2.2	0.45
F	-1	All cations	4	0.25
Hg	2	S	4.0	0.50
K	1	Halogen	9.0	0.112
Li	1	Halogen	5.3	0.188
Mg	2	O	5.98	0.334
Na	1	Halogen	6.7	0.15
O	-2	All cations	4	0.50
Rb	1	Halogen	9.8	0.102
Si	4	O	4.00	1.00
Sr	2	O	8.57	0.233
Ti	4	O	5.96	0.67
Tl	1	Halogen	8.3	0.120
Zn	2	O	4.98	0.402

diagrams of organic chemistry. For binary compounds and ternary compounds with coordination numbers less than ~ 8 , the observed bond graph can often be correctly generated using only the chemical formula together with a knowledge of the valences and typical coordination numbers of each atom. Cation coordination numbers are determined by both size and the bonding characteristics of the anions, but it is simpler to start with the assumption that the coordination number of each cation will be close to the average of the coordination numbers observed in many different compounds, as given by Brown (1988). The initial choice of coordination number is not critical, as the constraints encountered during the subsequent construction of the bond graph may require the coordination to change. From N , the average coordination number of an atom, one can make a first estimate of the valence S of the bonds it forms using

$$S = V/N. \quad (4)$$

S is referred to as the bonding strength of the atom and leads to an important theorem, the valence-matching principle, which states:

Since the valence of a bond will be close to the bonding strength of both the cation and the anion that form the bond, bonds are most likely to form between anions and cations with similar bonding strengths.

The average observed coordination numbers and bonding strengths of selected atoms are given in Table 1. One further principle is needed in constructing the bond graph and finding its mapping into three-

dimensional space. This is the principle of maximum symmetry, which can be written as:

At each stage in modelling a structure, symmetry is only broken when required by either the chemical or the spatial constraints.

In other words, wherever there is a choice to be made, the most symmetric solution consistent with the constraints should be chosen.

To construct a bond graph from the chemical formula, the bonding strengths S of the atoms are calculated and bonds are first drawn between the cations and anions with the highest bonding strength, the values of S being used to determine the cation coordination numbers. The first set of bonds will often link some of the atoms into a complex (often an anionic complex) whose bonding strength relative to other atoms in the structure can be calculated in the same way as the bonding strength of an atom. The process is then repeated until the graph is complete. At this point the coordination number of each atom should be close to its average coordination number and the bond valences should be close to the bonding strengths of the terminal atoms. The process is illustrated in the examples discussed below.

Once completed, the bond graph can be used to determine the multiplicity of each chemically distinct atom (*i.e.* the number of times it appears in the bond graph) and its maximum possible site symmetry, assigned by looking for the most symmetric arrangement of its bonds in space. This step is simplified by recognizing that since the structure eventually has to be mapped into a space group where all atoms will occupy Wyckoff positions, only the 32 crystallographic point groups given in *International Tables for Crystallography* (1983, Vol. A) need be considered. The principle of maximum symmetry further implies that bond graphs will be preferred in which the coordination environments of the atoms can have high crystallographic symmetry, namely the 12-coordinate cuboctahedron ($m\bar{3}m$), the eight-coordinate cube ($m\bar{3}m$), the six-coordinate octahedron ($m\bar{3}m$), the four-coordinate tetrahedron ($\bar{4}3m$) and (less favourably) the three-coordinate triangle ($\bar{6}2m$). Such high site symmetry may not always be attainable and useful listings of the subgroups compatible with triangular, tetrahedral and octahedral arrangements of bonds are given in Tables 2, 3 and 4, respectively, together with the elements of the site symmetry that the ligands inherit from the central atom.

SrTiO_3 , which stands as the aristotype* of the large class of perovskite and perovskite-related structures illustrates the way in which the principle of maximum symmetry can be used to generate a bond graph. The average observed coordination number for Sr^{2+} sur-

Table 2. *Subgroups for trigonal planar coordination*

Column 1 gives the order of the site symmetry of the central three-coordinate atom. Column 2 gives the site symmetry of the central atom. Column 3 gives the minimum site symmetries of the ligands, the superscript giving the number of symmetry-related ligands with this site symmetry. The ligand symmetry may be higher than that shown if the ligand also lies on symmetry elements that do not intersect the position of the central atom.

Order	Central atom site symmetry	Minimum site symmetries and multiplicities of the ligands
12	$\bar{6}2m$	$mm2^3$
6	32	2^3
	$\bar{6} (= 3/m)$	m^3
	$3m$	m^3
3	3	1^3
2	2	$2 + 1^2$
	m	$m + 1^2$
1	1	$1 + 1 + 1$

Table 3. *Subgroups for tetrahedral coordination*

For an explanation see Table 2.

Order	Central atom site symmetry	Minimum site symmetries and multiplicities of the ligands
24	$\bar{4}3m$	$3m^4$
12	23	3^4
8	$42m$	m^4
6	$3m$	$3m + m^3$
4	4	1^4
	222	1^4
	$mm2$	$m^2 + m^2$
3	3	$3 + 1^3$
2	2	$1^2 + 1^2$
	m	$m + m + 1^2$
1	1	$1 + 1 + 1 + 1$

rounded by O is 8.57 and for Ti^{4+} is 5.96 (Table 1). The bond graph (Fig. 1) is constructed by drawing first the strong bonds from Ti [$S = 0.67$ valence units (v.u.)] to O ($S = 0.50$ v.u.). According to the principle of maximum symmetry the Ti—O bonds should be distributed so as to leave the three O atoms equivalent. This is achieved with the expected coordination number of 6 if Ti forms two bonds to each of the three O atoms.

The way of adding the Sr—O bonds is less obvious and three possibilities are shown in Fig. 1. Eight-coordination is close to the average observed coordination number of Sr and is compatible with a high site symmetry ($m\bar{3}m$), providing all the Sr—O bonds are equivalent, but Fig. 1(a) shows that this equivalence is lost in the bond graph. Nine-coordination, which is also close to the average observed coordination number, maintains the equivalence of the nine Sr—O bonds in the bond graph (Fig. 1b), but there is no crystallographic site symmetry that allows all nine bonds to be equivalent. Only 12-coordination around Sr allows all the bonds to be equivalent in both the bond graph and the crystallographic site symmetry. Fig. 1(c) shows the preferred (and observed) bond graph in which the maximum possible point symmetry of Sr is $m\bar{3}m$. The

* An aristotype is defined here as a structure with high symmetry that has the same topology as a lower-symmetry observed structure. The observed structure can be thought of as derived from the aristotype by loss of symmetry through relatively small displacements of the atoms.

Table 4. Subgroups for octahedral coordination

For an explanation see Table 2.

Order	Central atom site symmetry	Minimum site symmetries and multiplicities of the ligands
48	$m\bar{3}m$	$4mm^6$
24	432	4^6
	$m\bar{3}$	$mm2^6$
16	$4/mmm$	$4mm^2 + mm2^4$
12	$\bar{3}m$	m^6
	23	$1^3 + 1^3$
8	$42m$	$4^2 + 2^4$
		$4^2 + m^4$
	422	$4^2 + 2^4$
	$4mm$	$4^2 + m^4$
	$4/m$	$4^2 + m^4$
	$m\bar{3}m$	$mm2^2 + m^4$
		$mm2^2 + mm2^2 + mm2^2$
6	32	1^6
	$\bar{3}$	1^6
4	4	$1 + 1 + 1^4$
	4	$4 + 4 + 1^4$
	222	$2^2 + 1^4$
		$2^2 + 2^2 + 2^2$
	$mm2$	$mm2 + mm2 + 1^4$
		$m^2 + m^2 + m^2$
	$2/m$	$m^2 + 1^4$
		$m^2 + m^2 + 2^2$
3	3	$1^3 + 1^3$
2	2	$2 + 2 + 1^2 + 1^2$
	m	$m + m + 1^2 + 1^2$
		$m + m + m + m + 1^2$
1	1	$1 + 1 + 1 + 1 + 1 + 1$

bond graph is completed using (2) and (3) to predict the bond valences and (1) to convert these to the chemically ideal bond lengths shown in Fig. 1.

This example shows how, in favourable cases, many of the properties expected for a structure, e.g. the bond graph, the coordination numbers, the ideal bond lengths and the ideal site symmetries of the atoms, can be determined from a bond-valence analysis of the chemical formula. According to the principle of maximum symmetry, one would expect these properties to be preserved as the bond graph is mapped into the crystal structure, although spatial constraints and electronic affects such as stereoactive lone pairs may require a lowering of the site symmetry of the atoms and a consequent straining of the bonds.

3. Crystallographic constraints

Crystallographic constraints appear when the finite bond graph is mapped into an infinite three-dimensional crystal. While it should be possible to map most bond graphs into the space group $P1$, the principle of maximum symmetry suggests that the highest, not the lowest, symmetry space groups will be preferred and that the space group $P1$ will only be adopted if it is impossible to map the structure into any space group of higher symmetry.

Shubnikov (1922), in his fundamental law of crystallography, pointed out that every atom in the formula unit (bond graph) of a crystal must occupy a general or special position (Wyckoff position) in one of the 230 three-dimensional space groups listed in *International Tables for Crystallography* (1983, Vol. A), but atoms of the bond graph can only be mapped into the Wyckoff positions of a space group if the atoms and Wyckoff positions have compatible multiplicities and symmetries. For example, the graph of $SrTiO_3$ shown in Fig. 1(c) requires a space group with at least two Wyckoff positions of multiplicity 1 to accommodate the Sr and Ti atoms and one Wyckoff position of multiplicity 3 to accommodate the three O atoms. Further, the maximum site symmetry allowed by the bond graph for Sr (12-coordinate cuboctahedron) and Ti (six-coordinate octahedron) is $m\bar{3}m$. The ideal space group is therefore one which has at least two Wyckoff positions of multiplicity 1 with site symmetry $m\bar{3}m$ and at least one site of multiplicity 3. The space group $Pm\bar{3}m$ (space-group number 221) is the only one that meets these conditions and it is the space group in which $SrTiO_3$ crystallizes.

The properties of the space groups, in particular the multiplicities and site symmetries of the various Wyckoff positions, are listed in *International Tables for Crystallography* (1983, Vol. A). However, for the purpose of embedding the bond graph into the space group a different set of multiplicities is needed, since symmetry elements that contain translations (lattice translations, glide planes and screw axes) do not give rise to special positions and therefore do not impose any constraints on the Wyckoff positions. All translational elements are therefore ignored and only the pure rotational and inversion operators are retained. These operations define a

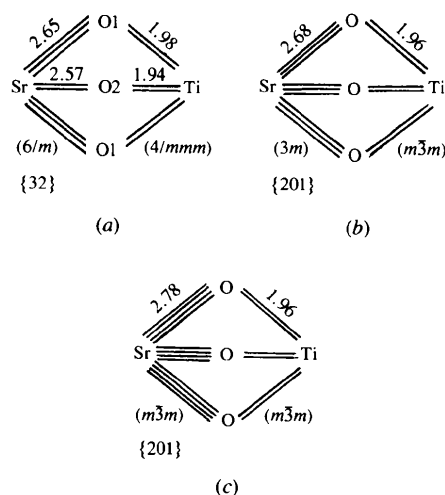


Fig. 1. Possible bond graphs of $SrTiO_3$ showing the spectrum of the bond graph, predicted bond lengths in Å and maximum site symmetry: (a) eight-coordinate Sr; (b) nine-coordinate Sr; (c) 12-coordinate Sr.

portion of the unit cell, in general, smaller than the primitive cell but larger than the asymmetric unit, in which the Wyckoff (*a*) position usually has a multiplicity of 1. For example, if the translational symmetry elements of the space group *Fddd* (70) are ignored, the multiplicities given in *International Tables for Crystallography* (1983, Vol. A) are all divided by 8. In this case the multiplicity of the (*a*) site is not 8, as given in *International Tables for Crystallography* (1983, Vol. A), but 1. Unless otherwise stated, the term 'multiplicity' is used only in this sense in the rest of this paper.

The non-translational order of a space group (O_s) is defined here as the number of symmetry-related atoms generated by the non-translational symmetry operations. It is, therefore, equal to the general position multiplicity (in the sense defined above). The order of the site symmetry of a Wyckoff position (O_w) is defined as the number of ways these same symmetry operations transform the site into itself. Since the symmetry operations that do not transform a Wyckoff position into itself are used to generate the symmetry-related sites, the product of the order of the site symmetry of a Wyckoff position and its multiplicity (M_w) is equal to the non-translational order of the space group

$$M_w O_w = O_s. \quad (5)$$

An important corollary of this equation is that atoms occupying sites of the same multiplicity must have crystallographic site symmetries of the same order. This places severe restrictions on the symmetries of the sites that can be occupied. In the hypothetical bond graph of MgSiO_3 , shown in Fig. 2, the Si atom has been given its expected coordination number of 4 (see Table 1), destroying the equivalence of the three O atoms and breaking them into two groups, O1 and O2, with Si bonded to two atoms of each group. The highest site symmetry for a tetrahedron with two inequivalent pairs of ligands can be found from Table 3, which shows that most site symmetries compatible with tetrahedral coordination require all four, or at least three, ligands to be crystallographically equivalent. The bond graph of Fig. 2 is only compatible with site symmetries *mm2* and 2 (ligand multiplicities 2 + 2), *m* (ligand multiplicities 1 + 1 + 2) or 1 (ligand multiplicities 1 + 1 + 1 + 1). The principle of maximum symmetry requires that we choose the highest of these site symmetries, *mm2*. Table 3 then shows that the ligands O1 and O2 must each lie on one of the mirror planes and hence have site symmetries of at least *m*.† Since the order of *mm2* is 4, the space group cannot have a non-translational order greater than 4. Assuming, following the principle of maximum symmetry, that the non-translational order is 4, (5) shows that O1 must have a site symmetry of the order 2, hence, from Table 3, its site symmetry can

only be *m*, while O2 must have a site symmetry of the order 4, thus its site symmetry can only be *mm2* or *2/m* (*International Tables for Crystallography*, 1983, Vol. A). Since Mg has the same multiplicity as Si, its site symmetry will also be of the order 4 which, from Table 4, shows that its site symmetry must be $\bar{4}$, 4, 222, *mm2* or *2/m*. However, only *mm2* and *2/m* allow O1 to have the site symmetry *m* determined above.

As an assistance to finding space groups with matching Wyckoff multiplicities, Galiulin & Khachaturov (1994) proposed using a space-group spectrum consisting of a list of ten numbers, giving the number of crystallographically distinct atoms that can be accommodated in Wyckoff positions having multiplicities of 1, 2, 3, 4, 6, 8, 12, 16, 24 and 48, respectively. For example, the spectrum of *Pm* $\bar{3}$ *m* is {2020***0**}, since it can accommodate two atoms each in sites of multiplicity 1 and 3, none in sites of multiplicity 2, 4 and 16 and an indefinite number in sites of multiplicity 6, 8, 12, 24 and 48, the latter sites having free positional parameters which allow them to accommodate more than one crystallographically distinct atom. A list of the spectra of all 230 space groups in order of decreasing symmetry is given in the *Appendix*, together with the site symmetries of the Wyckoff positions of multiplicity 1.

A spectrum can also be written for the bond graph of a compound. For SrTiO_3 the spectrum is {2010000000}, or {201} if the trailing zeros are omitted, since its bond graph (Fig. 1c) contains two atoms of multiplicity 1 (Sr and Ti) and one of multiplicity 3 (O). A space group will have Wyckoff positions of the right multiplicity if the numbers in its spectrum are at least as large as the corresponding numbers in the spectrum of the bond graph. Examination of the space-group spectra in the *Appendix* shows, for example, that SrTiO_3 cannot crystallize in either of the space groups *Im* $\bar{3}$ *m* or *Fm* $\bar{3}$ *m* as their spectra do not match. *Im* $\bar{3}$ *m* can only accommodate one atom in Wyckoff positions of multiplicity 1 and *Fm* $\bar{3}$ *m* has no positions of multiplicity 3. The *Appendix* can therefore be used to reduce the list of candidate space groups to those whose spectra match the spectrum of the bond graph.

Returning to the example of MgSiO_3 shown in Fig. 2, the search for a space group is narrowed to one with non-translational order 4, a spectrum compatible with {31} and site symmetries of *mm2* (for Si), *mm2* or *2/m* for Mg and O1, and *m* for O2. There are 15

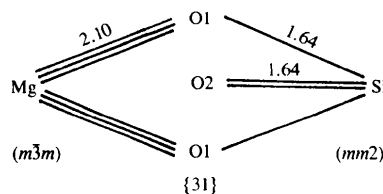


Fig. 2. The predicted bond graph of MgSiO_3 .

† Their site symmetry may be higher than this, but in any case it must include the mirror plane that passes through Si.

matches to be found using the *Appendix and International Tables for Crystallography* (1983, Vol. A). These must be individually examined to see which, if any, can accommodate the bond graph. This examination is not trivial as there are many parameters that need to be chosen to complete the mapping in low-symmetry space groups. However, the analysis shows that either the crystal has low symmetry (non-translational order of 4 or less) or that it has a different bond graph, possibly containing more than one formula unit. In fact, MgSiO_3 crystallizes in the pyroxene structure with a doubled formula unit, $\text{Mg}_2\text{Si}_2\text{O}_6$, and a different bond graph, suggesting that there is no satisfactory embedding for the bond graph of Fig. 2.

In the above analysis it has been assumed that the bond graph contains only one formula unit, as implied by the principle of maximum symmetry. However, structures such as pyroxene are known in which the graph contains more than one formula unit. In some of these cases the multiplicities of the atoms may have a common factor higher than 1. For a complete analysis such multiple formula unit graphs also should be examined, but they will generally have lower symmetry than the simple structures, since the quantity that measures the degree of symmetry is the non-translational order of the space group divided by the highest common factor of the multiplicities. In the interests of brevity, such multiple structures are not systematically examined here.

4. Mapping the bond graph into the space group

The previous section shows how the multiplicities and the coordination environments of atoms in the bond graph place severe restrictions on the space groups into which the graph can be embedded, but finding a space group that matches the multiplicity and symmetry of the atoms does not guarantee that an embedding is possible. Several further conditions must be satisfied. The lattice parameters and the coordinates of the atomic positions must be chosen in such a way that the expected bonds can be formed without bringing two anions or two cations into too close contact or leaving large open spaces in the structure. Some space groups will generate structures that are only connected in two-dimensions (layer structures) or one-dimension (fibrous structures) and there may be chemical reasons for passing over these in favour of a three-dimensionally connected structure. Not only must the expected bonds be formed, but their lengths should correspond to the lengths predicted by the network equations. Some bond strain is allowed, but if deviation between the ideal and observed bond lengths is too large, the structure will be unstable and will either not exist or will distort by lowering the symmetry.

For high-symmetry structures the number of free parameters that need to be chosen is usually small and a satisfactory model, if one exists, can easily be found. As

the symmetry is lowered, the number of free parameters increases, making it more difficult to find an embedding. The problem may be approached in two ways. Each candidate space group may be examined in turn and parameters chosen by trial and error, to see if a fit can be found, or the topology can be systematically expanded, starting at one of the atoms and taking explicit account of the chemical and symmetry constraints at each step. Both approaches break down at the lowest symmetries, where symmetry provides few constraints and the number of free parameters becomes large. For the large number of compounds that can form no high-symmetry structures, a different, as yet undiscovered, approach is needed.

It is easy to select the parameters for the perovskite structure of SrTiO_3 , because its high symmetry allows only one adjustable parameter, the cubic lattice parameter, a . Even though there are two possible ways of assigning the atoms to Wyckoff positions, only one gives the correct bond graph and all the atom coordinates are fixed by symmetry. The single adjustable parameter must be chosen to fit at least two chemical constraints, namely the Sr—O and the Ti—O bond lengths. In general this cannot be done, as the Sr—O bond must be equal to $a/2^{1/2}$ and the Ti—O bond must equal $a/2$. By chance, both these conditions are satisfied for SrTiO_3 where the Sr—O bond (valence = 2/12) is predicted to have a length of 2.78 Å and the Ti—O bond (valence = 4/6) is predicted to have a length of 1.96 Å, leading to predictions for a of 3.93 and 3.92 Å, respectively (observed 3.90 Å). However, this relationship between the bond lengths is not satisfied for BaTiO_3 and CaTiO_3 , since Ba and Ca are larger and smaller, respectively, than Sr. The Ba and Ca compounds accommodate the strain by distorting. The topology is essentially retained but, because the crystallographic symmetry is lowered, some bonds are broken and bonds that were equivalent in $Pm\bar{3}m$ are no longer equivalent in the lower-symmetry space group. While the cubic perovskite structure remains the aristotype for a large group of ABO_3 compounds, in almost all cases the failure of the ideal bond lengths to obey the geometric constraints leads to a lowering of the symmetry, as discussed in some detail by Woodward (1997a,b).

The approach described above can be used to derive many of the standard structure types in a systematic way, as shown in the examples that follow, but where a compound is found to adopt a structure of lower symmetry than that suggested by the analysis it is instructive to enquire after the cause. It may be the result of lattice strains, as in the example of the perovskites given above, or it may be electronic in origin, such as the Jahn–Teller distortion found around Cu^{2+} or the lone-pair effect found around Pb^{2+} . An ideal structure derived using the above analysis thus provides a reference to which the observed structure can be compared, helping to identify the various chemical or spatial constraints that are at work in the crystal.

5. Examples

The ideas developed above are illustrated by a number of examples which show how the chemical and spatial constraints combine to restrict, or in some cases determine, the possible structure.

5.1. NaCl, CsCl and ZnO

The simplest compounds are the binary salts which crystallize in the NaCl, CsCl, sphalerite and wurtzite (ZnO) structure types and whose bond graphs, including the spectra, maximum site symmetries and ideal bond lengths are given in Fig. 3. According to the principle of maximum symmetry, only coordination numbers of 4, 6, 8 and 12 need initially be considered. The *Appendix* is searched for space groups with spectra compatible with {2} and site symmetries of $m\bar{3}m$ (six-, eight- and 12-coordination) or $4\bar{3}m$ (four-coordination). Matches for $m\bar{3}m$ symmetry are found in only two space groups, $Fm\bar{3}m$ (225) and $Pm\bar{3}m$ (221), which generate the NaCl and CsCl structures with coordination numbers of 6 and 8, respectively. Matches for $4\bar{3}m$ symmetry are found in two other space groups, $Fd\bar{3}m$ (227) and $F4\bar{3}m$ (216), which correspond to the NaCl and sphalerite structures, respectively. The first of these has eight-coordination, but the ligands of each atom consist of four cations and four anions at the same distance, an arrangement that is only likely to be found in intermetallic compounds. $F4\bar{3}m$ gives a structure with tetrahedral coordination. As Niggli (1918–1919) pointed out, these are the only possible simple cubic structures with the formula AB and none has coordination number 12. The structure adopted by a given compound will depend on its average observed coordination number. Examples of a number of binary compounds are shown in Table 5, which compares the observed lattice parameters with those calculated using (1)–(3). Only structures for which bond-valence parameters for (1) are available are included in this table.

Although ZnO is known with the sphalerite structure, it normally crystallizes with the hexagonal wurtzite structure which can be found by continuing the search to lower-symmetry space groups. The next lowest subgroup for the site symmetry of tetrahedrally coordinated Zn is

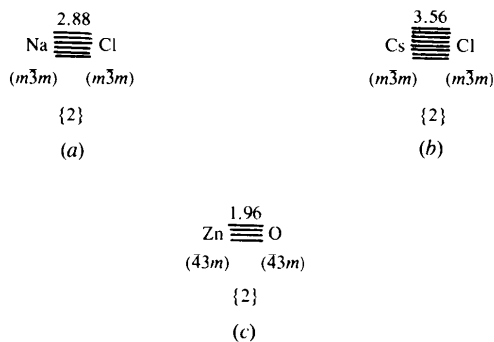


Fig. 3. Bond graphs of AB compounds: (a) NaCl, (b) CsCl and (c) ZnO.

Table 5. Predicted and observed lattice parameters

The lattice parameters are calculated from the predicted bond lengths shown in the table and on the figures. All distances are in Å. The selection of compounds is determined by the availability of the bond-valence parameters needed in (1).

	Bond length	<i>a</i> (calculated)	<i>a</i> (observed)	Average observed coordination number (from Table 1)
CsCl-type $Pm\bar{3}m$				
CsCl	3.56	4.11	4.12	Cation coordination = 8 10.4
TlI	3.59	4.14	4.20	8.3
NaCl-type $Fm\bar{3}m$				
LiF	2.02	4.04	4.02	Cation coordination = 6 5.3
NaF	2.34	4.68	4.62	6.7
KF	2.66	5.32	5.35	9.0
NaCl	2.88	5.76	5.64	6.7
KCl	3.18	6.36	6.29	9.0
RbCl	3.32	6.64	6.58	9.8
MgO	2.10	4.20	4.21	5.98
CaO	2.37	4.74	4.81	7.31
SrO	2.52	5.04	5.16	8.57
BaO	2.69	5.38	5.52	10.24
CdO	2.31	4.62	4.70	6.14
Sphalerite $F\bar{4}3m$				
ZnO	1.96	4.53	4.62	Cation coordination = 4 4.98
CdS	2.56	5.92	5.83	4.6
HgS	2.56	5.92	5.86	4.0
Wurtzite $P6_3mc$				
ZnO	1.96	3.22 (a)* 5.23 (c)*	3.25 5.21	Cation coordination = 4 4.98
Corundum $R\bar{3}c$				
Al ₂ O ₃	1.88	4.60 (a)* 13.00 (c)*	4.76 13.00	Cation coordination = 6 5.27
Fluorite $Fm\bar{3}m$				
CaF ₂	2.36	5.45	5.46	Cation coordination = 8 7.31
Anatase $I4_1/amd$				
TiO ₂	1.96	3.92 (a)* 7.98 (c)*	3.78 9.49	Cation coordination = 6 5.96
Rutile $P4_2/mnm$				
TiO ₂	1.96	4.73 (a)* 2.77 (c)*	4.59 2.96	Cation coordination = 6 5.96
Perovskite $Pm\bar{3}m$				
SrTiO ₃	1.96 (Ti) 2.78 (Sr)	3.92	3.90	Cation coordinations = 6 and 12 5.96 8.57

* Lattice parameters calculated assuming a regular cation coordination sphere.

23 (order 12, see Table 3), which yields five matching space groups but no new structures. In order 8, where the point group of Zn is $4\bar{2}m$, there are ten matching space groups which generate two new structures, one a layer structure with square-planar coordination [$P4_2/mcm$ (132)] and one a fibrous structure with linear two-coordination [$P4/nmm$ (129)]. A new tetrahedrally coordinated structure only appears in the space groups of non-translational order 6 with Zn site symmetry $3m$ and the first matching space group listed in the *Appendix* is $P6_3mc$ (186), the space group of the wurtzite structure

(Table 5). This analysis illustrates just how restrictive the spatial requirements can be. Only three simple non-metallic binary AB structures, one for each coordination number, are compatible with the 68 highest-symmetry space groups. Only if the search is continued further does the wurtzite structure appear, but even this apparently high-symmetry structure already has three free parameters and two formula units in the primitive unit cell.

Other AB structures are, of course, possible and will be found for compounds such as CuO and PbO , where electronic effects are expected to reduce the site symmetries or where the bond graph contains more than one formula unit. However, the failure of an AB structure to crystallize in one of the simple high-symmetry forms is a warning that additional constraints are present.

5.2. Al_2O_3

Two possible bond graphs of Al_2O_3 are shown in Fig. 4. Al with an average coordination number of 5.26 can be either six- or four-coordinated and each of these possibilities will be considered. First consider six-coordination, which is favoured because it not only gives a high-symmetry graph (Fig. 4a), but also because it results in Al—O bonds exactly equal to 0.50 v.u., the bonding strength of O. The spectrum of this graph is $\{011\}$, which means that the orders of the crystallographic site symmetries of Al and O are in the ratio 3:2 and, according to (5), the non-translational order of the space group must be a multiple of both 3 and 2. If the symmetry of the bond graph is to be maintained in the crystal, the possible space groups are restricted to those of non-translational order 48, 24, 12 and 6, and the site symmetries of Al are restricted to those listed in Table 4 with orders 24, 12, 6 and 3. There are no matching spectra in the *Appendix* for space groups with non-translational order 48 and only one, $Pn\bar{3}m$ (224), of order 24 that has a site symmetry for Al of 23 or $\bar{3}m$.* This, like the four matching space groups of order 12 (all cubic) and the two matching cubic space groups of the order 6, describe a defect fluorite structure in which the octahedral environment of Al is distorted. A number of cubic phases of Al_2O_3 are known (Zhou & Snyder, 1991), but these are disordered defect spinel structures that are best thought of as intermediate stages along the dehydration reaction pathway of AlOOH . Because they are disordered and the Wyckoff positions are not fully occupied, these phases cannot be found by the present method. There are eight matching hexagonal space groups of the order 6, but these all give structures with columns of face-sharing octahedra or trigonal prisms in which the cation-cation repulsions across the shared faces would lead to excessive strain. Not until

$R\bar{3}c$ (167) does one reach the observed space group of corundum, $\alpha\text{-Al}_2\text{O}_3$, whose calculated and observed lattice parameters are given in Table 5. Even though each AlO_6 octahedron shares one face with a neighbour, the structure is possible because the Al atoms are small and can move away from the shared face, but if Al is replaced by a larger cation face sharing is no longer possible. In this case the bixbyite structure is found. Even though bixbyite is cubic, its space group $Ia\bar{3}$ has the same non-translational order as $R\bar{3}c$, but the structure has a lower symmetry than corundum since its bond graph contains two, not one, formula units.

An analysis of the tetrahedral graph of Al_2O_3 illustrated in Fig. 4(b) shows why a high-symmetry tetrahedrally coordinated structure is unlikely. The spectrum is $\{12\}$ and the multiplicity, 2, of the Al atom requires that the non-translational order of the space group be twice the order of the site symmetry of Al. Further, since the bond graph shows that the Al—O2 bond is not equivalent to the three Al—O1 bonds, the site symmetry of Al must allow for at least one crystallographically inequivalent bond. Table 3 shows that the only site symmetries for Al with this property are $3m$ (order 6), 3 (order 3), m (order 2) and 1 (order 1). Thus, only space groups with non-translational order 12, 6, 4 and 2 need to be considered. There are matches for five space groups of non-translational order 12, but all of these require Al and O2 to lie on the same threefold axis and O1 to lie on a parallel threefold axis, an arrangement which gives a double-layer structure related to those found

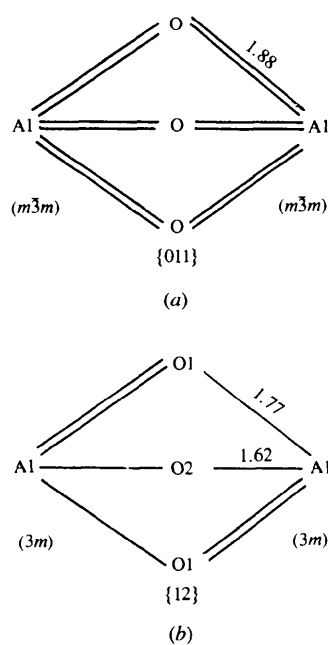


Fig. 4. Bond graphs for Al_2O_3 : (a) six-coordinate and (b) four-coordinate.

* Since only the site symmetries of the positions of multiplicity 1 are given in the *Appendix*, it is necessary to consult *International Tables for Crystallography* (1983, Vol. A) to obtain this information.

in layered silicates. This is a possible structure, but layer structures result in anion-anion contacts between the layers, a condition that is not favoured by small non-polarizable anions such as oxygen. Space groups of non-translational order 6 lead to similar structures. There are, however, many matching space groups of non-translational order 4 and 2 and, although it is possible that an embedding of the graph might be found among these, symmetry no longer provides enough constraints to guide the way. We can conclude that if tetrahedral Al_2O_3 exists and it does not have a layer structure, it will form a structure in a space group of non-translational order 1, 2 or 4 or it will have a more complex bond graph than that shown in Fig. 4(b).

5.3. CaF_2 , TiO_2 , CdCl_2 , CdI_2 and CaCl_2

The simple binary AB_2 compounds represented by CaF_2 , in which the Ca is eight-coordinated, and TiO_2 , CdCl_2 , CdI_2 and CaCl_2 in which the cation is six-coordinated, have one of the bond graphs shown in Fig. 5. Both graphs have the same spectrum, $\{11\}$, and the same maximal site symmetry around the cation ($m\bar{3}m$, order 48), but only CaF_2 has a compatible symmetry around the anion ($\bar{4}3m$, order 24).

The search for candidate space groups for CaF_2 starts with space groups of non-translational order 48 and immediately yields a match with $Fm\bar{3}m$ (225), which is the observed space group. The calculated and observed lattice parameters are given in Table 5.

In the bond graph of TiO_2 , representing the six-coordinate structures, the maximum symmetry around three-coordinate O is $\bar{6}2m$ (order 12, see Table 2), implying that the order of the site symmetry of Ti, and the non-translational order of the space group, cannot exceed 24. The highest site symmetry of Ti is, therefore, 432 or $m\bar{3}$ (Table 4), but the two matching space groups with this order yield only the CaF_2 structure and the 10 of the order 12 give either tetrahedral coordination around Ti or one of the layer structures, CdCl_2 ($R\bar{3}m$, 166) or CdI_2 ($P\bar{3}m1$, 164), which are stabilized by the more polarizable halide ions. Layer structures are not expected for TiO_2 , making it necessary to look further to space groups of non-translational order 8, where the first matching space group $I4_1/amd$ (141) is the space group of the anatase form of TiO_2 . The next two space groups listed in the Appendix, $I4/mcm$ (140) and $P4_2/nmc$ (137), provide matching Wyckoff positions, but do not allow an

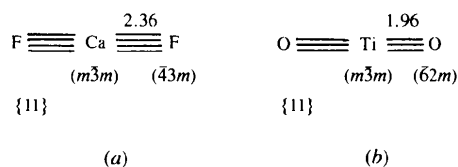


Fig. 5. Bond graphs of AB_2 structures: (a) CaF_2 and (b) TiO_2 .

embedding of the graph. However, the following space group does and $P4_2/mnm$ (136) is the space group of the rutile polymorph which has the same topology as the lower symmetry CaCl_2 . Although the anatase and rutile structures of TiO_2 can thus be readily derived, neither symmetry arguments nor the calculated lattice constants shown in Table 5 would suggest that rutile is stabilized by its higher density, nor would these arguments suggest the existence of the low-symmetry polymorph brookite, which has the space group $Pbca$ (61, non-translational order 2). Significantly, brookite is only stabilized by the presence of impurities.

5.4. $\text{Ca}_3\text{Al}_2(\text{SiO}_4)_3$

The formula $\text{Ca}_3\text{Al}_2(\text{SiO}_4)_3$ seems an unlikely candidate for a high-symmetry structure, but a high-symmetry bond graph can be drawn if Ca and Si have coordination numbers 4 or 8 and Al coordination number 6 (Fig. 6). Equation (5) shows that the site symmetry orders of Ca, Al and Si cannot be larger than 16, 24 and 16, respectively. No space groups with non-translational order 48 or 24 match both the spectrum $\{0120001\}$ and

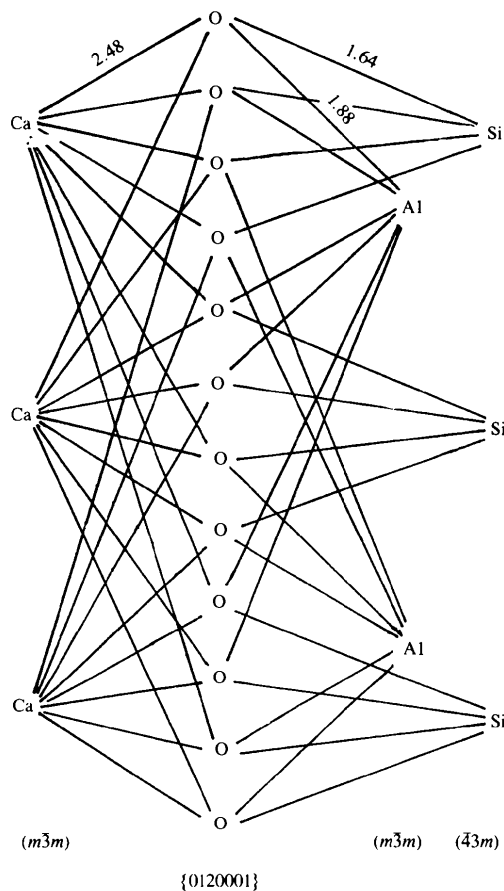


Fig. 6. The bond graph of $\text{Ca}_3\text{Al}_2(\text{SiO}_4)_3$.

the symmetry, and only in order 12 is there a matching space group, $Ia\bar{3}d$ (230), which can also accommodate the bond graph. Because the O atom in this space group occupies the general position, the structure has four free parameters [$a, x(O), y(O), z(O)$], which must be matched to the constraints provided by the Ca—O, Al—O and Si—O bond lengths and the expected tetrahedral angles at Si. Although the structure is technically overdetermined, it is still able to accommodate a range of different cations without distorting to a lower symmetry.

6. Discussion

The above discussion shows that both the chemical and the spatial constraints play an important role in deciding which structures, and hence which compounds, can exist. The need to match the chemical properties of an inorganic compound with the crystallographic properties of the space into which it is to be mapped provides severe constraints on the possible topologies that can be adopted. The relationship between the non-translational order of the space group and the multiplicity and site symmetry of the Wyckoff positions given by (5), when combined with the multiplicities and site symmetries predicted by the bond graph, reduces to a relatively manageable size the number of space groups that need to be considered. Not all these candidate space groups will allow an embedding of the bond graph

and, even where they do, it may not be possible to choose structural parameters that reproduce the predicted interatomic distances.

In favourable cases, however, this analysis does allow the local topology described by the bond graph to be unambiguously expanded into a high-symmetry three-dimensional structure. In other cases it will generate a small number of structures, *e.g.* layer and framework structures, which can be examined for their chemical plausibility. In still other cases, no structures of high or moderate symmetry will be found and, although it is not then possible to determine the structure directly, the reasons for the low symmetry are clear and the number of space groups that need to be considered is severely limited.

In some cases the analysis can provide a reference structure with which the observed structure can be compared. The failure of a compound to crystallize in the structure with the highest possible symmetry suggests that there are features of the structure or the chemistry that have been overlooked. For example, $BaTiO_3$ and $CaTiO_3$ do not crystallize in the space group $Pm\bar{3}m$ because of lattice strain and TiO_2 does not crystallize with the $CdCl_2$ structure because of the low polarizability of the O atoms. Contrary to expectation, it is not necessary to ask why $CdCl_2$ does not adopt the rutile structure since the $CdCl_2$ is the structure of higher symmetry.

APPENDIX

Space-group spectra

Spectra for all space groups arranged in order of decreasing symmetry. The symmetries of sites with multiplicity 1 are given at the end of each line followed by structure types that crystallize in the space group. (Site symmetries in parentheses refer to positions of multiplicity 2.)

Space groups of non-translational order 48

		1	2	3	4	6	8	12	16	24	48	Site symmetry	Example
229	$Im\bar{3}m$	1	0	1	1	*	*	*	0	*	*	$m\bar{3}m$	
225	$Fm\bar{3}m$	2	1	0	0	*	*	*	0	*	*	$m\bar{3}m$	NaCl, CaF_2
221	$Pm\bar{3}m$	2	0	2	0	*	*	*	0	*	*	$m\bar{3}m$	$CsCl$, $SrTiO_3$

Space groups of non-translational order 24

		1	2	3	4	6	8	12	16	24	Site symmetry	Example
227	$Fd\bar{3}m$	2	2	0	*	*	0	*	0	*	$\bar{4}3m$	NaI
226	$Fm\bar{3}c$	2	0	2	0	*	*	*	0	*	$\bar{4}32, m\bar{3}$	
224	$Pn\bar{3}m$	1	2	1	*	*	0	*	0	*	$\bar{4}3m$	
223	$Pm\bar{3}n$	1	0	1	1	*	*	*	0	*	$m\bar{3}$	
222	$Pn\bar{3}n$	1	0	1	1	*	*	*	0	*	432	
217	$I\bar{4}3m$	1	0	1	*	*	0	*	0	*	$\bar{4}3m$	
216	$F\bar{4}3m$	4	0	0	*	8	0	*	0	*	$\bar{4}3m$	ZnS
215	$P\bar{4}32$	2	0	2	*	*	0	*	0	*	$\bar{4}3m$	
211	$I432$	1	0	1	1	*	*	*	0	*	43	
209	$F432$	2	1	0	0	*	*	*	0	*	43	
207	$P432$	2	0	2	0	*	*	*	0	*	43	
204	$Im\bar{3}$	1	0	1	1	*	*	*	0	*	$m\bar{3}$	
202	$Fm\bar{3}$	2	1	0	0	*	*	*	0	*	$m\bar{3}$	
200	$Pm\bar{3}$	2	0	2	0	*	*	*	0	*	$m\bar{3}$	
191	$P6/mmm$	2	*	2	*	*	0	*	0	*	6/mmm	

APPENDIX (cont.)

Space groups of non-translational order 16

		1	2	3	4	6	8	12	16	Site symmetry
139	$I4/mmm$	2	*	0	*	0	*	0	*	$4/mmm$
123	$P4/mmm$	4	*	0	*	0	*	0	*	$4/mmm$

Space groups of non-translational order 12

		1	2	3	4	6	8	12	Site symmetry	Example
230	$Ia\bar{3}d$	0	2	2	*	*	0	*	$(\bar{3}, 32)$	Garnet
228	$Fd\bar{3}c$	1	2	1	*	*	0	*	23	
219	$F4\bar{3}c$	2	0	2	*	*	0	*	23	
218	$P4\bar{3}n$	1	0	3	*	*	0	*	23	
210	$F4_232$	2	2	0	*	*	0	*	23	
208	$P4_232$	1	2	3	*	*	0	*	23	
203	$Fd\bar{3}$	2	2	0	*	*	0	*	23	
201	$Pn\bar{3}$	1	2	1	*	*	0	*	23	
197	$I32$	1	0	0	*	*	0	*	23	
196	$F23$	4	0	0	*	*	0	*	23	
195	$P23$	2	0	2	*	*	0	*	23	
194	$P6_3/mmc$	4	*	*	0	*	0	*	$\bar{3}m, \bar{6}2m$	
193	$P6_3/mcm$	2	*	*	*	*	0	*	$\bar{3}m, \bar{6}2m$	
192	$P6/mcc$	2	*	2	*	*	0	*	$\bar{6}2, 6/m$	
189	$P\bar{6}2m$	2	*	*	*	*	0	*	$\bar{6}2m$	
187	$P6m2$	6	*	*	0	*	0	*	$\bar{6}2m$	
183	$P6mm$	*	*	*	0	*	0	*	$6mm$	
177	$P622$	2	*	2	*	*	0	*	622	
175	$P6/m$	2	*	2	*	*	0	*	$6/m$	
166	$R\bar{3}m$	2	*	2	0	*	0	*	$\bar{3}m$	$CdCl_2$
164	$P\bar{3}m1$	2	*	2	0	*	0	*	$\bar{3}m$	CdI_2
162	$P\bar{3}1m$	2	*	2	*	*	0	*	$\bar{3}m$	

Space groups of non-translational order 8

		1	2	3	4	6	8	Site symmetry	Examples
141	$I4_1/amd$	2	*	0	*	0	*	$42m$	Anatase
140	$I4/mcm$	4	*	0	*	0	*	$422, \bar{4}2m, 4/m, mmm$	
137	$P4_2/nmc$	2	*	0	*	0	*	$42m$	
136	$P4_2/nmm$	2	*	0	*	0	*	mmm	Rutile
134	$P4_2/nm$	2	*	0	*	0	*	$42m$	
132	$P4_2/mcm$	4	*	0	*	0	*	$42m, mmm$	
131	$P4_2/mmc$	6	*	0	*	0	*	$42m, mmm$	
129	$P4/nmm$	*	*	0	*	0	*	$42m, 4mm$	
128	$P4/nmc$	2	*	0	*	0	*	$4/m$	
127	$P4/mbm$	4	*	0	*	0	*	$4/m$	
126	$P4/nnc$	2	*	0	*	0	*	42	
125	$P4/nbm$	4	*	0	*	0	*	$42m, 42$	
124	$P4/mcc$	2	*	0	*	0	*	$4/m, 42$	
121	$I\bar{4}2m$	2	*	0	*	0	*	$42m$	
119	$I4m2$	4	*	0	*	0	*	$42m$	
115	$P4m2$	4	*	0	*	0	*	$42m$	
111	$P\bar{4}2m$	4	*	0	*	0	*	$42m$	
107	$I4mm$	*	*	0	*	0	*	$4mm$	
99	$P4mm$	*	*	0	*	0	*	$4mm$	
97	$I422$	2	*	0	*	0	*	42	
89	$P422$	4	*	0	*	0	*	42	
87	$I4/m$	2	*	0	*	0	*	$4/m$	
83	$P4/m$	4	8	0	*	0	*	$4/m$	
71	$Immm$	4	*	0	*	0	*	mmm	
69	$Fmmm$	2	*	0	*	0	*	mmm	
65	$Cmmm$	4	*	0	*	0	*	mmm	
47	$Pmmm$	8	*	0	*	0	*	mmm	

APPENDIX (cont.)

Space groups of non-translational order 6

		1	2	3	4	6	Site symmetry	Examples
213	$P4_132$	2	*	*	0	*	32	
212	$P4_332$	2	*	*	0	*	32	
206	$Ia\bar{3}$	2	*	*	0	*	$\bar{3}$	Bixbyite
205	$Pa\bar{3}$	2	*	0	0	*	$\bar{3}$	
199	$I2_13$	0	*	8	0	*	(3)	
190	$P6_2c$	4	*	*	0	*	32	
188	$P6c2$	6	*	*	0	*	32	
186	$P6_3mc$	*	0	*	0	*	3m	Wurtzite
185	$P6_3cm$	*	*	*	0	*	3m	
184	$P6cc$	*	*	*	0	*	6	
182	$P6_322$	4	*	*	0	*	$\bar{3}, \bar{6}$	
176	$P6_3/m$	2	*	*	0	*	$\bar{3}, \bar{6}$	
174	$P6$	6	*	*	0	*	$\bar{6}$	
168	$P6$	*	*	*	0	*	6	
167	$R\bar{3}c$	2	*	*	0	*	3, 32	Corundum
165	$P\bar{3}c1$	2	*	*	0	*	3, 32	
163	$P\bar{3}1c$	4	*	*	0	*	$\bar{3}, 32$	
160	$R3m$	*	0	*	0	*	3m	
157	$P\bar{3}1m$	*	*	*	0	*	3m	
156	$P\bar{3}m1$	*	0	*	0	*	3m	
155	$R32$	2	*	*	0	*	32	
150	$P321$	2	*	*	0	*	32	
149	$P312$	6	*	*	0	*	32	
148	$R\bar{3}$	2	*	2	0	*	$\bar{3}$	
147	$P\bar{3}$	2	*	2	0	*	$\bar{3}$	

Space groups of non-translational order 4

		1	2	3	4	Site symmetry		1	2	3	4	Site symmetry	
181	$P6_422$	4	*	0	*	222	75	$P4$	*	*	0	*	4
180	$P6_222$	4	*	0	*	222	74	$Imma$	*	*	0	*	2/m
142	$I4_1/acd$	2	*	0	*	$\bar{4}, 222$	72	$Ibam$	4	*	0	*	222
138	$P4_2/ncm$	*	*	0	*	$\bar{4}, 2/m, 222, mm2$	70	$Fddd$	2	*	0	*	222
135	$P4_2/mbc$	4	*	0	*	$\bar{4}, 2/m, 222$	68	$Ccca$	2	*	0	*	222
133	$P4_2/nbc$	4	*	0	*	$\bar{4}, 222$	67	$Cmma$	*	*	0	*	2/m
130	$P4/ncc$	*	*	0	*	$\bar{4}, 222$	66	$Ccca$	6	*	0	*	222
122	$I4_2d$	2	*	0	*	$\bar{4}$	64	$Cmca$	2	*	0	*	2/m
120	$I4c2$	4	*	0	*	$\bar{4}, 222$	63	$Cmcm$	*	*	0	*	2/m
118	$P4n2$	4	*	0	*	$\bar{4}, 222$	59	$Pmmn$	*	*	0	*	mm2
117	$P4b2$	4	*	0	*	$\bar{4}, 222$	58	$Pnnm$	4	*	0	*	2/m
116	$P4c2$	4	*	0	*	$\bar{4}, 222$	55	$Pbam$	4	*	0	*	2/m
114	$P4_21c$	2	*	0	*	$\bar{4}$	53	$Pmna$	4	*	0	*	2/m
113	$P4_21m$	*	*	0	*	$\bar{4}, mm2$	51	$Pmma$	*	*	0	*	2/m, mm2
112	$P4_2c$	6	*	0	*	$\bar{4}, 222$	50	$Pban$	4	*	0	*	222
109	$I4_1md$	*	*	0	*	mm2	49	$Pccm$	8	*	0	*	2/m
108	$I4cm$	*	*	0	*	$\bar{4}, mm2$	48	$Pnnn$	4	*	0	*	222
105	$P4_2mc$	*	*	0	*	mm2	44	$Imm2$	*	*	0	*	mm2
104	$P4nc$	*	*	0	*	4	42	$Fmm2$	*	*	0	*	mm2
103	$P4cc$	*	*	0	*	4	38	$Amn2$	*	*	0	*	mm2
102	$P4_2nm$	*	*	0	*	mm2	35	$Cmm2$	*	*	0	*	mm2
101	$P4_2cm$	*	*	0	*	mm2	25	$Pmm2$	*	*	0	*	mm2
100	$P4bm$	*	*	0	*	$\bar{4}, mm2$	23	$I222$	4	*	0	*	222
98	$I4_122$	2	*	0	*	222	22	$F222$	4	*	0	*	222
94	$P4_22_12$	2	*	0	*	222	21	$C222$	4	*	0	*	222
93	$P4_222$	6	*	0	*	222	16	$P222$	8	*	0	*	222
90	$P4_212$	*	*	0	*	$\bar{4}, 222$	12	$C2/m$	4	*	0	*	2/m
88	$I4_1/a$	2	*	0	*	$\bar{4}$	10	$P2/m$	4	*	0	*	2/m
86	$P4_2/n$	2	*	0	*	$\bar{4}$							
85	$P4/n$	*	*	0	*	$\bar{4}, 4$							
84	$P4_3/m$	6	*	0	*	2/m						Site symmetry	
82	$I4$	4	*	0	*	$\bar{4}$			1	2	3		
81	$P4$	4	*	0	*	$\bar{4}$	198	$P2_13$	*	0	*	3	
79	$I4$	*	*	0	*	4	173	$P6_3$	*	0	*	3	

Space groups of non-translational order 3

APPENDIX (cont.)

		1	2	3	4	Site symmetry			1	2	Site symmetry
161	<i>R3c</i>	*	0	*		3	56	<i>Pccn</i>	*	*	$2, \bar{1}$
159	<i>P31c</i>	*	0	*		3	54	<i>Pcca</i>	*	*	$2, \bar{1}$
158	<i>P3c1</i>	*	0	*		3	52	<i>Pnna</i>	*	*	$2, \bar{1}$
146	<i>R3</i>	*	0	*		3	46	<i>Ima2</i>	*	*	$m, 2$
143	<i>P3</i>	*	0	*		3	45	<i>lba2</i>	*	*	2

Space groups of non-translational order 2

		1	2	Site symmetry			1	2	Site symmetry
179	<i>P6₅22</i>	*	*	2	37	<i>Ccc2</i>	*	*	2
178	<i>P6₁22</i>	*	*	2	36	<i>Cmc2₁</i>	*	*	<i>m</i>
172	<i>P6₄</i>	*	*	2	34	<i>Pnn2</i>	*	*	2
171	<i>P6₂</i>	*	*	2	32	<i>Pba2</i>	*	*	2
154	<i>P3₂21</i>	*	*	2	31	<i>Pmn2₁</i>	*	*	<i>m</i>
153	<i>P3₂12</i>	*	*	2	30	<i>Pnc2</i>	*	*	2
152	<i>P3₁21</i>	*	*	2	28	<i>Pma2</i>	*	*	$m, 2$
151	<i>P3₁12</i>	*	*	2	27	<i>Pcc2</i>	*	*	2
110	<i>I4₁cd</i>	*	*	2	26	<i>Pmc2₁</i>	*	*	<i>m</i>
106	<i>P4₂bc</i>	*	*	2	24	<i>I2₁2₁2₁</i>	*	*	2
96	<i>P4₃2₁2</i>	*	*	2	20	<i>C222</i>	*	*	2
95	<i>P4₃22</i>	*	*	2	18	<i>P2₁2₁2</i>	*	*	2
92	<i>P4₁2₁2</i>	*	*	2	17	<i>P222₁</i>	*	*	2
91	<i>P4₁22</i>	*	*	2	15	<i>C2/c</i>	*	*	$2, \bar{1}$
80	<i>I4₁</i>	*	*	2	14	<i>P2₁/c</i>	4	*	$\bar{1}$
77	<i>P4₂</i>	*	*	2	13	<i>P2/c</i>	*	*	$2, \bar{1}$
73	<i>lbca</i>	*	*	$2, \bar{1}$	11	<i>P2₁/m</i>	*	*	$m, \bar{1}$
62	<i>Pnma</i>	*	*	$m, \bar{1}$	8	<i>Cm</i>	*	*	<i>m</i>
61	<i>Pbca</i>	2	*	$\bar{1}$	6	<i>Pm</i>	*	*	<i>m</i>
60	<i>Pbcn</i>	*	*	$2, \bar{1}$	5	<i>C2</i>	*	*	2
57	<i>Pbcm</i>	*	*	$2, \bar{1}$	3	<i>P2</i>	*	*	2
					2	<i>P$\bar{1}$</i>	8	*	$\bar{1}$

Space groups of non-translational order 1

		1	Site symmetry			1	Site symmetry		1	Site symmetry	
170	<i>P6₅</i>	*	1	76	<i>P4₁</i>	*	1	7	<i>Pc</i>	*	1
169	<i>P6₁</i>	*	1	33	<i>Pna2₁</i>	*	1	4	<i>P2₁</i>	*	1
145	<i>P3₂</i>	*	1	29	<i>Pca2₁</i>	*	1	1	<i>P1</i>	*	1
144	<i>P3₁</i>	*	1	19	<i>P2₁2₁2₁</i>	*	1				
78	<i>P4₃</i>	*	1	9	<i>Cc</i>	*	1				

I wish to thank Hans Burzlaff for making me aware of the power and importance of space-group theory, Ravil Galiulin for suggesting the approach that has been developed in this paper, Vadim Urusov for drawing my attention to the work of Shubnikov and Niggli, a sceptical anonymous referee for keeping me honest and the Natural Science and Engineering Research Council of Canada for a research grant.

References

- Brese, N. E. & O'Keefe, M. (1992). *Acta Cryst.* **A48**, 663–669.
 Brown, I. D. (1988). *Acta Cryst.* **B44**, 545–553.
 Brown, I. D. (1992). *Acta Cryst.* **B48**, 553–572.
 Brown, I. D. & Altermatt, D. (1985). *Acta Cryst.* **B41**, 244–247.

Galiulin, R. V. & Khachaturov, V. R. (1994). *Mathematical Modelling of Composite Objects*, edited by V. R. Khachaturov, pp. 28–83. Communications in Applied Mathematics, Computing Centre of the Russian Academy of Sciences, Moscow.

International Tables for Crystallography (1983). Vol. A. Dordrecht: Kluwer Academic Publishers.

Niggli, P. (1918–1919). *Geometrische Kristallographie des Diskontinuums*. Leipzig: Gebr. Borntraeger.

Shubnikov, A. V. (1922). *Izv. Ross. Akad. Nauk*, **16**, 515–527.

A more accessible account of Shubnikov's Law is given by N. L. Smirnova & V. S. Urusov [*Comp. Math. Appl.* (1988), **16**, 563–567].

Woodward, P. M. (1997a). *Acta Cryst.* **B53**, 32–43.

Woodward, P. M. (1997b). *Acta Cryst.* **B53**, 44–66.

Zhou, R.-S. & Snyder, R. L. (1991). *Acta Cryst.* **B47**, 617–630.